Biochimica et Biophysica Acta 1817 (2012) 938–947

Contents lists available at SciVerse ScienceDirect

Biochimica et Biophysica Acta

journal homepage: www.elsevier.com/locate/bbabio

Review

The fictile coordination chemistry of cuprous-thiolate sites in copper chaperones ☆

M. Jake Pushie [a], Limei Zhang [a,b], Ingrid J. Pickering [a], Graham N. George [a,*]

[a] Department of Geological Sciences, University of Saskatchewan, 114 Science Place, Saskatoon, SK, Canada S7N5E2
[b] Present address: Division of Chemistry and Chemical Engineering, California Institute of Technology, Pasadena, CA, USA

ARTICLE INFO

Article history:
Received 16 August 2011
Received in revised form 6 October 2011
Accepted 14 October 2011
Available online 25 October 2011

Keywords:
Copper transport
Cuprous thiolate clusters
Copper homeostasis
EXAFS

ABSTRACT

Copper plays vital roles in the active sites of cytochrome oxidase and in several other enzymes essential for human health. Copper is also highly toxic when dysregulated; because of this an elaborate array of accessory proteins have evolved which act as intracellular carriers or chaperones for the copper ions. In most cases chaperones transport cuprous copper. This review discusses some of the chemistry of these copper sites, with a view to some of the structural factors in copper coordination which are important in the biological function of these chaperones. The coordination chemistry and accessible geometries of the cuprous oxidation state are remarkably plastic and we discuss how this may relate to biological function. This article is part of a Special Issue entitled: Biogenesis/Assembly of Respiratory Enzyme Complexes.

1. Introduction

Copper plays vital roles in the active sites of several enzymes essential for human health [1]. Cytochrome oxidase is among the most important of these enzymes; others include Cu–Zn superoxide dismutase which protects against oxidative damage, amine oxidases, and other metabolically important enzymes. Copper's biological usefulness depends in part upon its redox chemistry, since both Cu^{I} and Cu^{II} oxidation states are readily accessible under physiological conditions. Redox chemistry also may be responsible for the extreme toxicity of free copper ions, which are thought to generate cytotoxic reactive oxygen species through Fenton-type chemistry [2]. This chemistry may be exploited in the immune response, as elevated copper levels are found in phagosomes during activation of macrophages and phagocytosis [3]. Because of its toxicity, copper is one of the most tightly regulated metal ions, estimated to be present at less than one free copper ion in a typical cell, [4,5]. Specific trafficking pathways have evolved to ensure cellular copper is either compartmentalized or bound to protein carrier molecules, with multiple mechanisms protecting cells from copper toxicity [6].

Copper metallochaperones are small proteins which function in the intracellular trafficking of copper ions. These proteins face a particular chemical challenge — they must release their metal payload at their intended targets but must otherwise retain the bound metal with some tenacity in order to maintain homeostasis. Certain structural and chemical themes recur across the copper metallochaperones. X-ray crystallography and nuclear magnetic resonance (NMR), the two major tools for determining protein structure, have been applied extensively to the accessory proteins for cytochrome oxidase assembly. However, with notable exceptions copper chaperones tend to give up their bound copper on crystallization [7,8]. Thus, while the structure of the apo-proteins can be informative, there is often no direct information on the coordination of the metal. NMR can provide indications based on the chemical shifts of coordinating residues, but again direct and quantitative structural information on copper coordination is lacking. Because of these factors the technique of X-ray absorption spectroscopy has played a central role in developing an understanding of the structures of the metal sites. This review discusses the chemistry of these copper sites in the context of the structural factors in copper coordination which are important in the biological function of these chaperones.

2. Material and methods

Density functional theory (DFT) calculations employed $Dmol^3$ Materials Studio Version 5.5 [9,10]. Calculations used Becke exchange [11] and Perdew correlation [12] functionals both for the potential during the self-consistent field procedure, and for energy minimization during geometry optimization. Double numerical basis sets included polarization functions for all atoms. All calculations, including Cu^{I} and Cu^{II} complexes as well as organic ligands, were spin-unrestricted and used all-electron core potentials. Solvation effects were modeled using the Conductor-like Screening Model COSMO [13] in $Dmol^3$ with the dielectric value of water ($\varepsilon = 78.39$). Convergence was considered to be achieved when energies differed by less than 2×10^{-5} Hartree, the maximum force was less than 0.004 Hartree/Å and the maximum displacement was less than 0.005 Å. A

☆ This article is part of a Special Issue entitled: Biogenesis/Assembly of Respiratory Enzyme Complexes.

* Corresponding author. Tel.: +1 306 966 5683; fax: +1 306 966 8593.
E-mail address: g.george@usask.ca (G.N. George).

0005-2728/$ – see front matter © 2011 Elsevier B.V. All rights reserved.
doi:10.1016/j.bbabio.2011.10.004

maximum step size of 0.3 Å was used in the geometry optimizations. In most cases we expect interatomic distances for directly coordinated atoms computed by DFT to be within 0.05 Å of the true value, whereas accuracies for remote atoms will have larger values and will depend on the nature of the structure.

Analysis of X-ray absorption spectra used the EXAFSPAK suite of computer programs [14]. The extended X-ray absorption fine structure (EXAFS) oscillations $\chi(k)$ were quantitatively analyzed by curve-fitting as described by George et al. [15] with *ab initio* theoretical phase and amplitude functions calculated using the program FEFF version 8.25 [16–18].

3. Cuprous copper — a spectroscopically "silent" metal

The field of bioinorganic chemistry has been enormously enriched by spectroscopic studies of metal-containing active sites. Particularly informative have been UV–visible electronic spectroscopy, including circular dichroism and magnetic circular dichroism, and electron paramagnetic resonance and its various derivatives. Cuprous copper cannot be studied by these methods because it possesses a fully occupied outer shell of electrons ($3d^{10}$) and thus has been called a spectroscopically silent or quiet metal [19], a category which includes Cu^{I} and Zn^{II}. Copper has two stable magnetic isotopes, ^{63}Cu and ^{65}Cu, with 69% and 31% abundance, respectively. Both have $I = {}^{3}/_{2}$ with significant quadrupole moments, making observation of useful nuclear magnetic resonance spectra challenging, [20,21].

X-ray absorption spectroscopy (XAS) depends upon fundamental atomic properties and so can always be used to provide information on metal ion active sites, irrespective of their electronic structure. Furthermore, a unique benefit of XAS is that it requires no pre-treatment or extraction, and thus provides a tool that can probe chemical species *in situ*. X-ray absorption spectra arise from photo-excitation of a core electron, a 1s electron for a K-edge. The spectrum can be arbitrarily divided into two overlapping regions — the near-edge spectrum which is the structured region within approximately 50 eV of the absorption edge, and the extended X-ray absorption fine structure (EXAFS), comprising oscillations on the high-energy side of the absorption edge and which can be accurately interpreted in terms of a local radial structure [22] (Fig. 1).

Nomenclature of near-edge spectra is confused [22], but this region is often referred to as the X-ray absorption near-edge fine structure or XANES. The structure in near-edge spectra is due to transitions from the core level (1s for K-edge) to unoccupied molecular orbitals of the system. Intense dipole-allowed transitions ($\Delta l = \pm 1$) are observed for K-edge excitations to levels with a considerable *p*-orbital character. Near-edge spectra are therefore sensitive to electronic structure, giving a fingerprint of the chemical species of the metal or metalloid concerned. Fig. 2 shows the near-edge spectra of a series of different cuprous thiolate compounds. The advantage of the near-edge region of the spectrum is that it can be quickly collected with good signal to noise. In contrast to the near-edge, EXAFS is more difficult to collect with adequate signal to noise, and is not always practical for dilute samples. Some early applications of EXAFS suffered from over-interpretation of the data, but when used with appropriate caution EXAFS is very well suited to the study of metalloprotein active sites [22,23]. EXAFS can be understood by considering the photoelectron that arises from photo-excitation of the core electron as a de Broglie wave. This photoelectron wave will be scattered by nearby atoms, and because the initial state wave function (*e.g.* 1s for a K-edge) is very compact and centered at the absorber atom nucleus, the absorption depends to a good approximation upon the final state wave-function at the nucleus of the absorber atom. When the backscattered wave is in phase with the outgoing then the absorption is at a maximum whereas when it is out of phase it is at a minimum (this can imagined as constructive and destructive interference, respectively; Fig. 1). The de Broglie wavelength will decrease as the X-ray energy increases above the absorption edge and the phase at the nucleus thus changes as a function of incident X-ray energy, as well as being modulated by the absorber and backscatterer. The EXAFS manifests as an oscillation in the absorption, the frequency of which can be used to measure the separation of nearby atoms, and EXAFS can thus provide very accurate inter-atomic distances. The amplitude of the EXAFS oscillations is related to the number of nearby atoms and to their size (number of electrons, or atomic number). In essence the EXAFS can be analyzed to give the types (approximate atomic numbers) and distances of atoms that are near the absorber atom (Fig. 3).

Experimental EXAFS represents the backscattering from all the nearby atoms, and in some cases this can combine and give rise to

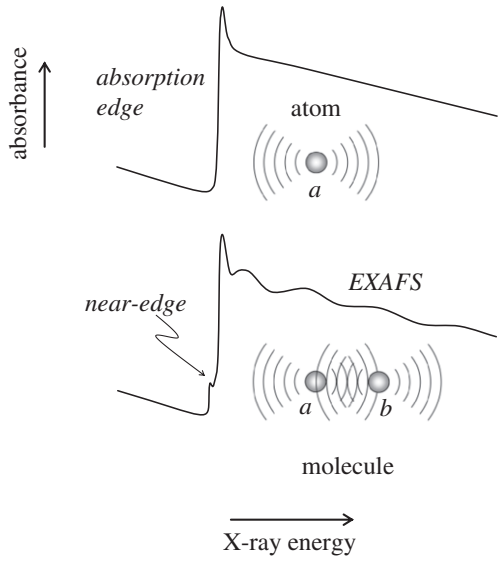

Fig. 1. Schematic diagram illustrating the physics of X-ray absorption spectroscopy. The upper diagram shows X-ray absorption by an atom whereas the lower absorption by a molecular species. The insets show the de Broglie photoelectron wave proceeding out from the absorber atom *a*, which in the case of the molecule is backscattered by a neighbor atom *b* giving rise to the extended X-ray absorption fine structure (EXAFS).

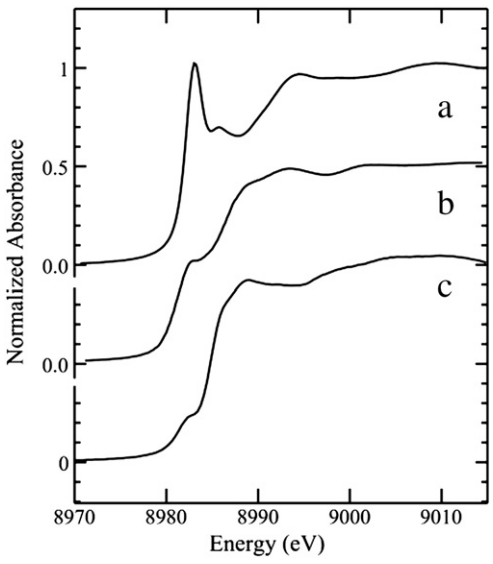

Fig. 2. Near-edge spectra of sulfur-coordinated cuprous species. *a* shows the spectrum of digonally coordinated $[Cu(SC_{10}H_{12})_2]^{2-}$, *b* that of the trigonally coordinated $[Cu_4(SPh)_6]^{2-}$, and *c* the spectrum of the four coordinate Cu^{I} site found in the orange protein from *Desulfovibrio gigas*.

a quite complex spectrum. Data is typically analyzed by fitting a theoretical model to the experimental data. EXAFS can provide very accurate interatomic distances R, usually ± 0.02 Å, and less accurate coordination numbers N, usually within 20%. EXAFS is usually displayed as a function of the photoelectron wave vector $k = \sqrt{\frac{2m_e}{\hbar^2}(E-E_0)}$, where E_0 is the threshold energy, and m_e the electron mass. The EXAFS $\chi(k)$ is defined as the oscillatory part of the absorption coefficient. It is dimensionless but is normally weighted by k^3 to counteract various losses in amplitude. The EXAFS resolution ΔR can be defined as the smallest difference in distance that can be distinguished with similar atoms (*e.g.* two different Cu–S interactions) and is approximately given by $R \approx \pi/2k$, where k is the extent of the data in $Å^{-1}$. For copper K-edge measurements the data may be truncated at $k = 13$ $Å^{-1}$ by traces of Zn in the sample (Zn K-edge excitation), and ΔR is thus close to 0.12 Å in such cases. EXAFS therefore does not have particularly good bond-length resolution. Given the correct arrangement of backscatterers EXAFS can also wholly or partially cancel. This final point is particularly important in EXAFS analysis of Cu–S clusters and is addressed below.

4. Copper and cytochrome oxidase assembly

Assembly of cytochrome oxidase requires a number of steps including both the assembly of subunits translated on both cytoplasmic and mitochondrial ribosomes, and the delivery and insertion of hemes and copper into the complex. Cytochrome oxidase contains several different metal sites and a total of three copper ions [24]. One, known as heme a_3-Cu_B, lies deep within the Cox1 subunit and is the site of O_2 reduction. Two more copper ions comprise the binuclear Cu_A center within the Cox2 subunit. Copper insertion into the Cox1 and Cox2 subunits is thought to occur within the mitochondrial inter-membrane space because the accessory proteins that are responsible for construction of the copper sites are located there. A number of proteins including Cox11, Cox17, Cox19, Cox23 and Sco1 are implicated in the biochemistry of copper incorporation [25]. Cox11 and Sco1 are associated with the mitochondrial inner membrane, but with a soluble domain lying within the inter-membrane space. Cox17 is a key copper metallochaperone within the inter-membrane space, donating cuprous copper to both Cox11 and Sco1 in yeast [26]. Cox17 can exist in two distinct conformers. One conformer apparently binds a single Cu^I ion stabilized by two disulfide bonds [27], while the other is an oligomeric complex coordinating a poly-copper thiolate cluster [28]. Detailed knowledge of the copper coordination in the monomeric conformer is currently lacking. While redox roles for some copper assembly proteins have recently been suggested [29,30], the cuprous oxidation state seems to play the central role in the function of most copper metallochaperones. Some of the relevant copper chemistry will now be discussed.

5. The fictile coordination chemistry of cuprous copper

5.1. Mononuclear copper complexes

Copper has three possible oxidation states which may all be accessible in biological systems: Cu^I, Cu^{II}, and Cu^{III}. The existence of percuprates, Cu^{III}, in biological systems remains questionable in many cases, due in part to the very high potentials needed for its generation in a strictly aqueous medium [31], and are not discussed further. Divalent or cupric copper is $3d^9$ and exhibits a highly characteristic and large Jahn–Teller distortion which means that most Cu^{II} complexes possess a tetragonally distorted octahedral coordination geometry. Distortion of Cu^{II} complexes away from a square planar type geometry is generally unfavorable energetically. For example, DFT calculations show that distorting $[(CH_3S)_4Cu^{II}]^{2-}$ from C_{4h} (square planar) to D_{2d} (pseudo-tetrahedral) geometry requires in excess of 80 kJ/mol. Cuprous copper however, with a $3d^{10}$ configuration, has no Jahn–Teller distortion and is thus much more forgiving of geometric distortions in its coordination geometry, compared with Cu^{II}. Complexes with digonal two-coordinate linear coordination, trigonal three coordinate planar coordination and pseudo tetrahedral geometries are known. Intermediate coordination geometries are also known, such as the T-shaped geometry in which copper has two shorter bonds subtending a bond-angle of less than 180° and one longer bond to a third ligand forming the stem of the T. In the case of cuprous ions with sulfur donors, some general rules may be derived by examining the small molecule structural literature using the Cambridge Structural Database (CSD) [32] and through DFT calculations. Each type of coordination (Fig. 4) has systematically different mean bond-lengths, with digonal linear at 2.17 Å, trigonal planar at 2.26 Å, and four coordinate pseudo-tetrahedral thioether bound species at

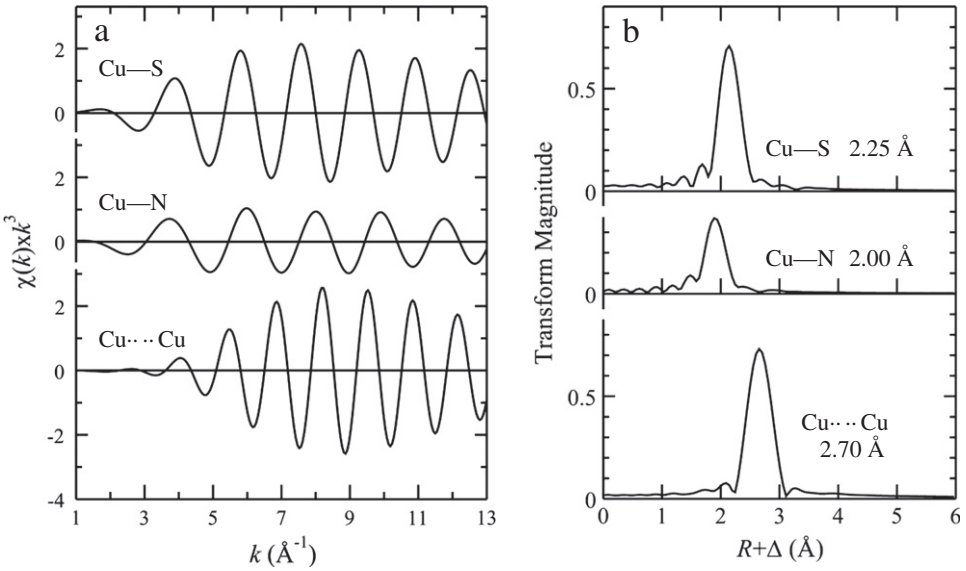

Fig. 3. Computed EXAFS spectra and EXAFS Fourier transforms for different absorber-backscatterer pairs. Transforms are phase-corrected for Cu – S backscattering. Physically realistic interatomic distances are used, and these are shown in the Fourier transform plots. It can be seen that the Fourier transforms give peaks at close to the interatomic distances.

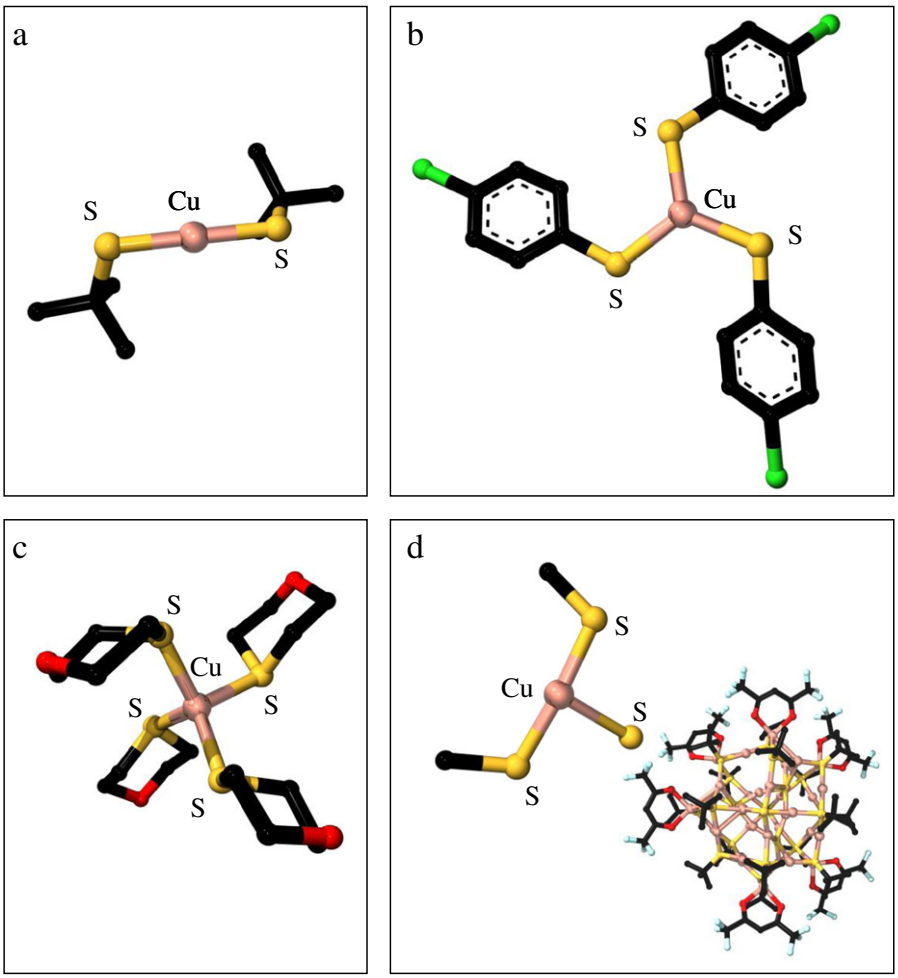

Fig. 4. Categories of cuprous ion coordination observed in small molecules. *a* shows the digonal complex tetraethylammonium *bis*(*t*-butylthiolato)-copper(i) $[(C_4H_9S)_2Cu](NEt_4)$ (CSD entry code KOBVAZ [33]), *b* the trigonal planar species *bis*(tetraethylammonium) *tris*(4-chlorophenylthiolato)-copper(i) (CSD entry code QUPXAA [34]), *c* a four coordinate species (CSD entry code BIZBIV01 [35]), and *d* a T-shaped site in the complex poly-copper structure shown in the inset (CSD entry code MEDBED [36]).

2.30 Å. The digonally coordinated species are reasonably rigid, with an energetic penalty of about 30 kJ/mol for an approximately 30° deviation from linearity (Fig. 5). The geometry optimized energy-minimized structures show a C–S–(Cu)–S–C torsion angle of close to 90°. This is due to the highest occupied molecular orbital being made up of orthogonal S 3p with Cu 3d contributions, although the energetic penalty of rotating away from this ideal angle is quite small (Fig. 5). Insofar as the T-shaped complexes are concerned (Fig. 4d), restricting our analysis to species with large S–Cu–S bond angles in the range 140–180°, then the two short Cu–S bonds range from 2.19 to 2.20 Å and the longer bonds from 2.29 to 2.67 Å [32]. The length of the long Cu–S bond approximately correlates with the short S–Cu–S bond angle (correlation coefficient ~0.7). Based on the number of entries in the CSD [32] and using the above definition of T-shaped species the most common coordination for cuprous thiolate is T-shaped, followed by digonal, with trigonal planar closely following in third place. In DFT geometry optimizations of isolated unconstrained mononuclear molecules T-shaped species invariably relax to trigonal planar species, and in agreement with this all CSD entries showing T-shaped complexes have some structural features that serve to distort the coordination from its true energy minimum.

Four coordinate cuprous complexes with sulfur donors are much rarer in the CSD than the other species discussed above. Most four coordinate species with sulfur donors have uncharged ligands such as substituted thiourea or related species. Restricting the searches to donors that resemble species related to biologically-relevant ligands, four coordinate cuprous ions are only observed with thioether donors (analogous to methionine; Fig. 4). There are no examples of four coordinate cuprous thiolate coordination compounds in the CSD, presumably because this type of coordination is too electron rich. Density functional calculations support this hypothesis, leading to the prediction that four coordinate cuprous thiolate complexes are not stable entities (not illustrated).

Investigating the relationship between three-coordinate T-shaped and trigonal planar species, we consider a hypothetical reaction between a methane thiolate and a digonal copper coordinated by two methane thiolates to form a trigonal planar complex:

$$CH_3S^- + \left[(CH_3S)_2Cu^I\right]^- \rightarrow \left[(CH_3S)_3Cu^I\right]^{2-}$$

Using DFT to map out the energy as the reaction proceeds (Fig. 6), the overall change in energy is a little more than 50 kJ/mol with a well-defined plateau that corresponds to a Cu–S bond-length range of 2.85 to 2.70 Å over which the energy only changes by a few kJ/mol. No well defined transition state can be found for this reaction. Thus, quite subtle thermodynamic differences between two and three coordinate copper make interchange of coordination geometry feasible. In agreement with this, most of the T-shaped geometries found in the small molecule literature are in species that have steric factors contributing to the strain on individual copper sites. The use of thiolate corresponds to basic conditions, as the pKa of a typical

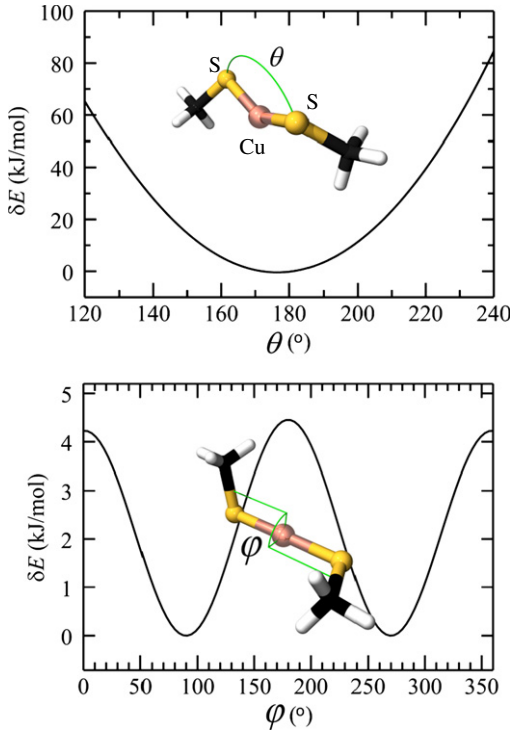

Fig. 5. Density functional theory calculations of the energetic dependence upon the S–Cu–S bond angle θ and the C–S–(Cu)–S–C torsion angle φ for the digonal species $[(CH_3S)_2Cu^I]^-$. Relative energies δE are given relative to the minimum computed energy.

aliphatic thiol is generally close to 8.3. The thermodynamics of the reaction of thiols depends subtly upon the nature of the species used to accept the proton. With imidazole as proton acceptor the reaction proceeds:

$$CH_3SH + \left[(CH_3S)_2Cu^I\right]^- + [C_3N_2H_4] \rightarrow \left[(CH_3S)_3Cu^I\right]^{2-} + [C_3N_2H_5]^+$$

Here a potential energy barrier of some 145 kJ/mol is computed with a well-defined transition state corresponding to a state in which the thiol proton has been abstracted by imidazole but thiolate has not yet reacted to form the trigonal complex (not illustrated). In a protein system a variety of factors may contribute to charge compensation and proton abstraction. Op't Holt and Merz have recently performed similar calculations using H_2O as a proton acceptor to form $[H_3O]^+$ [37] with conclusions similar to some of those discussed above.

5.2. Mononuclear mixed thiolate nitrogen-bound species

Mixed coordination types are found in some of the machinery of copper homeostasis such as the CsoR repressor [38] and in the cuprous form of Sco1 [39]. Examination of the CSD indicates that in small molecules with $Cu(SR)_2N$ coordination the geometry can vary from T-shaped species in which the Cu–N bond corresponds to the stem of the T, with a S–Cu–S bond-angle approaching 180°, to triangular type species analogous to trigonal planar coordination [32]. In T-shaped species the orientation of the Cu–N bond relative to the S–Cu–S moiety can also vary considerably, depending upon the nature of the complex. As with the T-shaped trigonal thiolate species complexes the Cu–N bond and the S–Cu–S bond angle are related; the longer the Cu–N bond the closer the bond-angle is to 180° (correlation coefficient ~0.7).

Taken together the above clearly shows that coordination chemistry of cuprous copper is highly plastic, or fictile. The energetic penalty for distortion from ideal geometries is quite small and the cuprous oxidation state is thus well suited to the purposes of biological metal transfer reactions which will require changes in metal ion coordination with minimal change or input of energy.

5.3. Cuprous thiolate clusters — a recurring structural motif

The established chemistry of cuprous thiolate clusters is very rich, with a large number of variations and types [*e.g.* 40]. Three possible cases are considered here: (*i*) binuclear Cu_2 complexes, (*ii*)

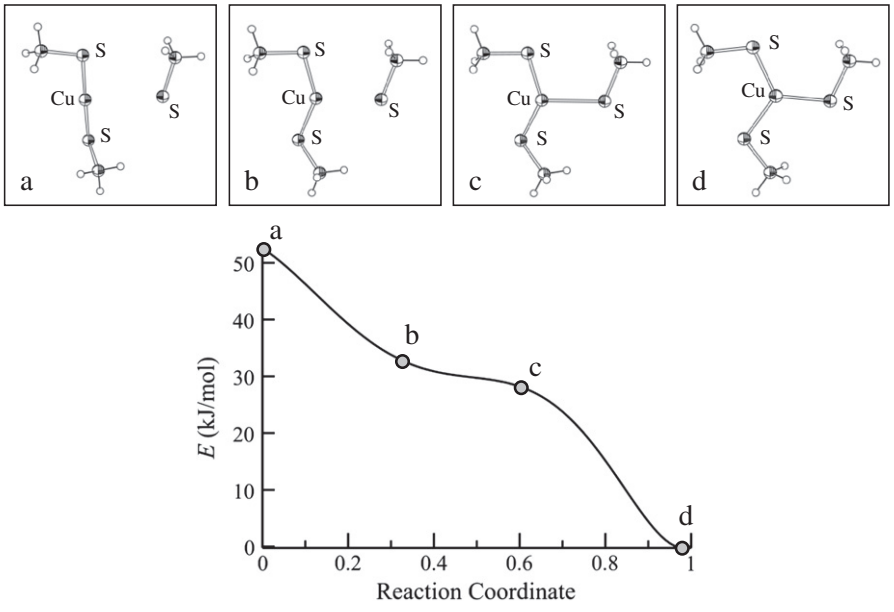

Fig. 6. Density functional theoretical calculations of a hypothetical reaction sequence for the digonally coordinated cuprous thiolate species $[(CH_3S)_2Cu^I]^-$ reacting with methanethiolate to produce the trigonal planar complex $[(CH_3S)_3Cu^I]^{2-}$ (C_{3h} point group symmetry). Structures (*a*–*d*) are shown for representative points on the potential energy curve (energies are relative to product *d*).

$[Cu_4(SR)_6]^{2-}$ clusters, and (*iii*) higher nuclearity clusters. Binuclear clusters of the form $[RS–Cu(SR)_2Cu–SR]^{2-}$ have been postulated to occur in biological systems [28,41]. Restricting results to those species with three-coordinate Cu^I ions, only a small number of binuclear Cu^I clusters are represented in the CSD and these fall into two types — those with approximate trigonal planar copper geometry [42] and those which are effectively comprised of two associated T-shaped complexes [43].

DFT calculations of $[CH_3SCu(SCH_3)_2CuSCH_3]^{2-}$ indicate that two different types of dimeric species with trigonal planar coordination are possible. The first has a planar core in which the bridging sulfurs and the metals all line in the same plane with a computed Cu···Cu distance of 2.72 Å. This structure has the methyls of the two bridging thiolates pointing alternately up and down from the Cu_2S_2 plane giving C_i point group symmetry (Fig. 7). There are no examples of this type of coordination in the CSD. The second dimeric structure lies at ~21 kJ/mol lower in energy than the first and can be thought of the first structure folded about the vector joining the two bridging sulfurs with the methyls on the same side of the folded Cu_2S_2 plane giving C_2 point group symmetry. This species has a computed Cu···Cu distance of 2.54 Å. The dimer of T-shaped species can be simulated by using C_2 symmetry with one S – Cu – S bond-angle constrained to 160°. Geometry optimizations gave a minimized energy differing from that of the folded trigonal planar dimer by only about 8 kJ/mol, indicating that binuclear clusters should be very flexible. The computed Cu···Cu distance is 2.65 Å for the dimer of T-shaped coordinated cuprous ions (Fig. 7). A planar-core dimer with C_i point group symmetry can also be calculated for T-shaped coordinated cuprous ions (again one S – Cu – S bond-angle constrained to 160°). This is only 1 kJ/mol above the trigonal Cu complex with a planar core and gives a longer Cu···Cu distance of 3.52 Å. The few available crystal structures give characteristic short Cu···Cu distances for the trigonal complex (2.58 Å [42,44]) and a variety of longer distances for the dimer of T-shaped species. The CSD contains many more entries for binuclear cuprous clusters with four coordinate copper, and Cu···Cu distances ranging from 2.59 to 3.53 Å are found. There is, however, no evidence for four-coordinate cuprous ions among the cytochrome oxidase accessory proteins.

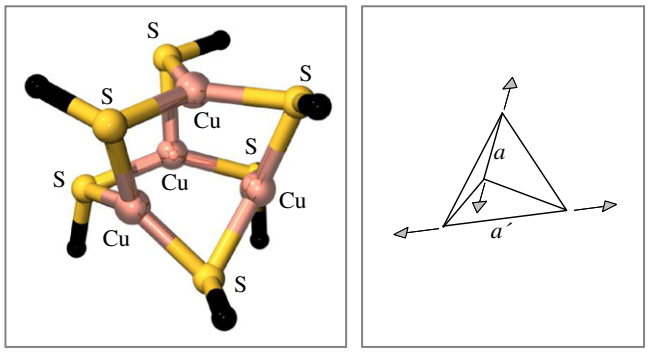

Fig. 8. Energy minimized geometry optimized density functional theory structure for the $[Cu_4(SCH_3)_6]^{2-}$ cluster with a schematic of the distortion from pure tetrahedral Cu_4 arrangement discussed in the text.

The clusters based on a $[Cu_4(SR)_6]^{2-}$ core are a common structural motif in chemistry. The structure of a typical $[Cu_4(SR)_6]^{2-}$ cluster can be visualized as a tetrahedron of Cu^I ions with the coppers separated by about 2.7 Å. Six bridging thiolates each coordinated to two Cu^I ions are positioned above each edge of the tetrahedron. In reality these clusters rarely approach the ideal regular geometry described above. A search of the CSD for distortions of $[Cu_4(SR)_6]^{2-}$ clusters indicates that distortions away from tetrahedral arrangement of copper ions is widespread, with a maximum and minimum range in Cu···Cu distances within individual clusters of 0.80 and 0.01 Å, respectively. A common distortion is for two out of the six Cu···Cu vectors to be elongated with respect to the others (Fig. 8). This has the effect of stretching the core in those directions, with a concomitant compression in another direction. This spread of distances means that analysis of the EXAFS can be somewhat problematic, as discussed below. Density functional calculations can be used to shed light on this apparent flexibility. Constraining two co-planar Cu···Cu vectors

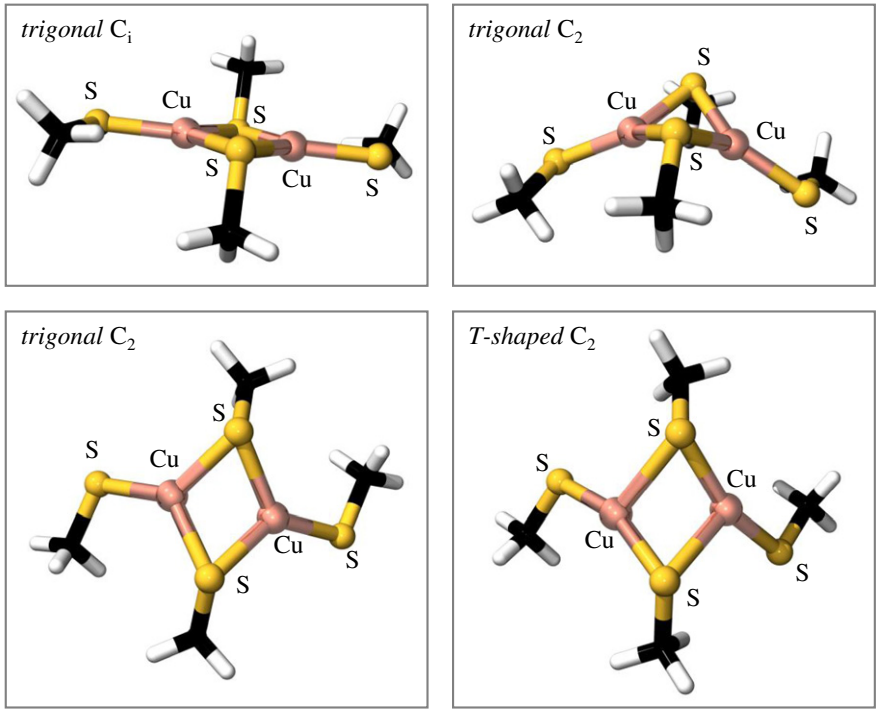

Fig. 7. Energy-minimized geometry-optimized density functional theory calculations of hypothetical copper dimeric species. The upper panels compare trigonally coordinated copper dimers with C_i and C_2 point group symmetry, the former having a planar CuS_2Cu core and the latter a folded core. The lower panels compare trigonal and T-shaped dimeric species for C_2 point group symmetry. All the complexes are close in energy.

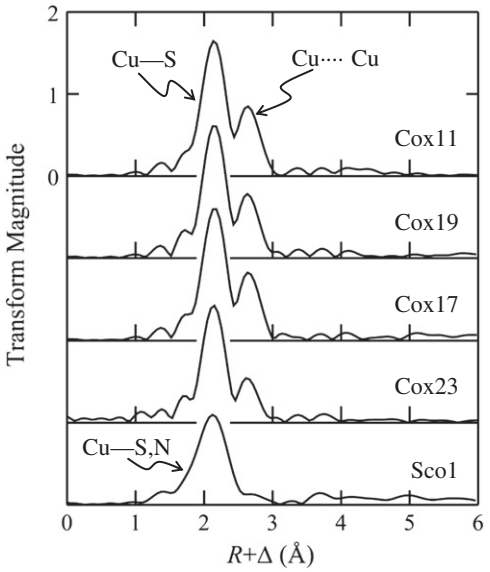

Fig. 9. EXAFS Fourier transforms of copper chaperones. The Cu – S phase-corrected EXAFS Fourier transforms of yeast Cox11 [41], Cox19 [49], Cox23 [25], Cox17 [28] and Sco1 [39] are compared. The observation of Cu···Cu backscattering in all but Sco1 indicates that these proteins are capable of forming poly-copper clusters, at least in the forms studied. The transforms were computed over the *k*-range 1.0 to 13.0 $Å^{-1}$.

to pre-defined distances (Fig. 8) and comparing the results of energy minimized geometry optimizations indicates that an increase of 0.15 Å in the two co-planar Cu···Cu vectors requires only a little more than 1 kJ/mol, whereas an increase of 0.25 Å requires about 5 kJ/mol. Proteins can exert significant distortions on a metal site with an energetic upper bound that is probably close to 100 kJ/mol. A good example is of such distortion is provided by the blue copper proteins such as stellacyanin (PDB ID 1JER) [45] for which DFT gives a difference of 65 kJ/mol between the equilibrium structure and the crystallographic geometry. Thus, the $[Cu_4(SR)_6]^{2-}$ cluster is a very pliable structural motif readily distorted by an enfolding protein, and because biological systems rarely show high symmetry the presence of distortions in biological clusters is not particularly surprising, if not expected.

Biological $[Cu_4(SR)_6]^{2-}$ clusters and related species have been suggested to occur in the yeast Ace1 and Mac1 transcription factors [46], the C-terminal domain of the yeast Ctr1 copper transporter [47], possibly in yeast Cox11 [41], in mammalian oligomeric Cox17 [48] and in yeast Cox19 [49]. Ace1 and Mac1 are not strictly part of the cytochrome c oxidase assembly system and thus are not directly relevant to this review. Nevertheless, they represent the best-studied examples of $[Cu_4(SR)_6]^{2-}$ type clusters in biology and are part of the overall copper homeostasis, and we will therefore discuss them briefly here. In the case of Ace1 and Mac1 small long-range features at about 3.7 Å were observed in the EXAFS. Such features are observed in $[Cu_4(SR)_6]^{2-}$ model species and arise from long range multiple scattering involving triangular paths that will be insensitive to the cluster distortions discussed above [46]. These small features require data with very good signal to noise, which is not always available for biological molecules. In addition to the cluster distortions discussed above, Brown et al. [46] also discussed a number of other possible distortions (such as twisting the cluster), and concluded that Mac1 and Ace1 probably possessed $[Cu_4(SR)_6]^{2-}$ type clusters rather than more compact forms [46]. Mac1 differs from Ace1 in that it lacks sufficient conserved cysteine residues to form $[Cu_4(Cys)_6]^{2-}$ instead having five such cysteines plus one conserved histidine. Brown et al. used DFT calculations to argue for a $[Cu_4(Cys)_5(His)]^{2-}$ with a histidine nitrogen bridging two coppers [46]. The binding of Cu-Ace1 to DNA was also investigated, and the cluster was found to show additional distortions when bound, although the 3.7 Å interactions remained essentially unchanged, suggesting that the distorted $[Cu_4(Cys)_6]^{2-}$ cluster was still intact. This distortion on binding DNA in turn suggests that the cluster is intimately associated with binding nucleic acid [46]. The $[Cu_4(SR)_6]^{2-}$ clusters in transcription factors also appear to be cooperatively assembled [46,50], so that the clusters form in an all-or-nothing manner and low copper loadings would result in $[Cu_4(SR)_6]^{2-}$ clusters in a fraction of the molecules. Similar $[Cu_4(SR)_6]^{2-}$ clusters are cooperatively assembled in yeast metallothionein under low copper loadings [51]. The formation of a poly-copper cuprous thiolate cluster in transcription factors allows the organization and stabilization of a larger structural unit than would a single metal ion. Moreover, the formation of the cluster undoubtedly confers a degree of metal ion specificity. For example, Ace1 is activated by Cu^{I} or Ag^{I} but not by other metal ions [52]. While cells will not normally be exposed to Ag^{I}, other physiologically relevant metal ions such as Zn^{II} will not form clusters of similar structure.

Fig. 9 shows a comparison of the EXAFS Fourier transforms of several yeast copper chaperones. In almost all cases the EXAFS analysis

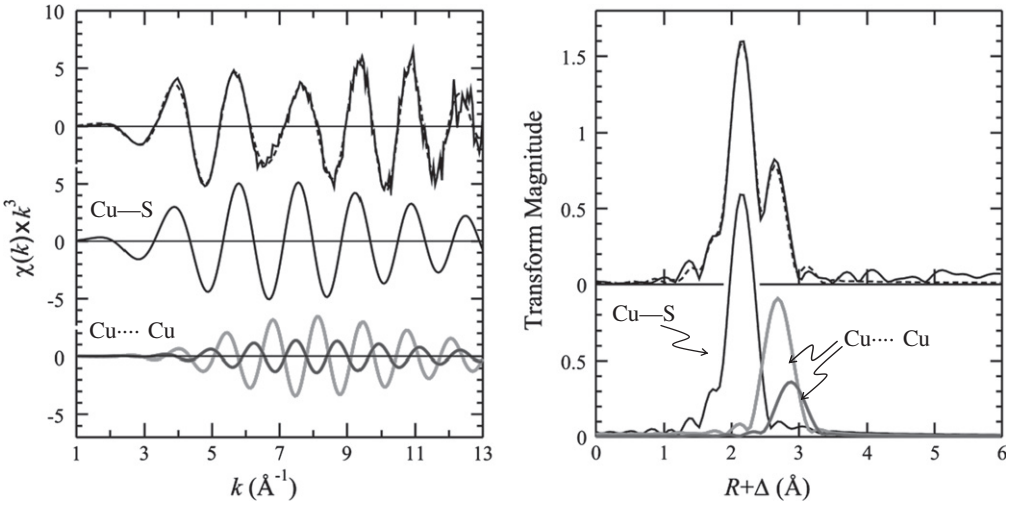

Fig. 10. EXAFS analysis of fully copper loaded yeast Cox17. The EXAFS (solid line) and the best fits (broken line) are shown together with the corresponding Cu – S phase-corrected EXAFS Fourier transforms. The parameters obtained from the best fits are summarized in Table 1. The figure shows the near-cancellation of Cu···Cu backscattering that can occur in poly-copper clusters.

Table 1
EXAFS curve-fitting of yeast Cox17.

Fit	Interaction	*N*	*R*	σ^2	ΔE_0	*F*
1	Cu – S	3	2.249 (2)	0.0049 (1)	−18.4 (5)	0.220
	Cu··Cu	1	2.705 (2)	0.0043 (2)		
2	Cu – S	3	2.255 (2)	0.0048 (1)	−16.8 (4)	0.212
	Cu··Cu	2	2.719 (2)	0.0067 (2)		
	Cu··Cu	1	2.917 (6)	0.0072 (2)		

Coordination numbers *N*, interatomic distances *R* (Å), Debye–Waller factors σ^2 (Å^2), and threshold energy shift ΔE_0 (eV). Values in parentheses are the estimated standard deviations obtained from the diagonal elements of the covariance matrix, which are precisions and are distinct from the accuracies which are expected to be larger (*ca* ±0.02 Å for *R*, and ±20% for *N* and σ^2). The fit-error function *F* is defined as $\sqrt{\sum k^6\left(\chi(k)_{calc}-\chi(k)_{expt}\right)^2 / \sum k^6 \chi(k)^2_{expt}}$, where the summations are over all data points in the *k*-range 1.0–13.0 Å^{-1}.

may be complicated by partial cancellation of at least two different Cu··Cu interatomic separations For example, the EXAFS of yeast Cox17 [28] is reproduced in Fig. 10, together with a re-analysis, summarized in Table 1. The data can be adequately fit by using either a single Cu··Cu interaction [28] or two different Cu··Cu interactions which partially cancel. The difference between the fit-error function of the two alternative fits is quite small (0.008), amounting to only about 4% of the total error (Table 1). Distinguishing between these two alternative fits is nontrivial. Use of standard statistical significance tests is not particularly useful as their application is not strictly valid in EXAFS analysis [53], and in many cases definitive determination of cluster type may not always be possible from analysis of the EXAFS. As previously discussed, fully reduced yeast Cox17 shows dimers and tetramers as major species with a copper binding stoichiometry of approximately three coppers per monomer [28], and a dimer could therefore potentially contain a $[Cu_4(SR)_6]^{2-}$ cluster. Moreover, the binuclear clusters tend to have shorter Cu··Cu distances, unless the planar higher energy conformation discussed above is involved.

As mentioned above, Cox17 can exist in a monomeric form which apparently binds a single Cu^I ion and is stabilized by two disulfide bonds [30]. At present, it seems likely that the Cox17 form relevant to copper transfer to Sco1 (which in turn transfers copper to the Cox2 Cu_A site) is the monomeric form. Voronova et al. have suggested that Cu_4Cox17 may play a physiological role in providing safe storage of excess copper in the mitochondrial inter-membrane space [48]. This poses the problem of whether removal of copper from the relatively stable $[Cu_4(SR)_6]^{2-}$ is practical in Cu_4Cox17. Metallothioneins can give up bound metal ions, and the fact that yeast metallothionein seems to cooperatively assemble a $[Cu_4(SR)_6]^{2-}$ cluster [51] indicates that at least in this system the cluster can fulfill a metal storage function. Recently, Blackburn and co-workers [29] have provided evidence

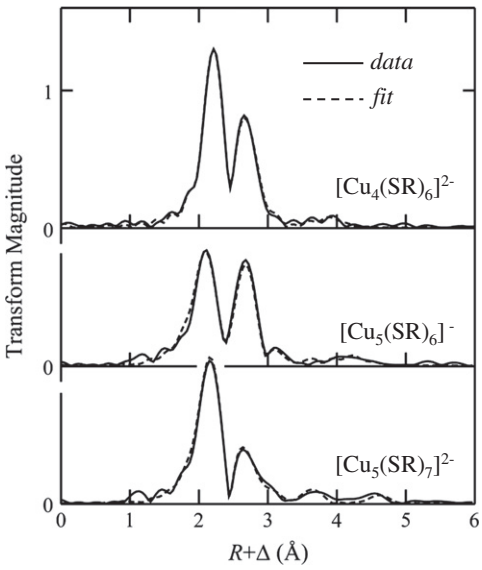

Fig. 12. Comparison of the Cu K-edge EXAFS Fourier transforms (solid lines) together with the results of EXAFS curve-fitting (broken lines) for [Cu4S6, Cu5S6 and Cu5S7]. Fits were computed using structural parameters taken from the crystal structures [54,57,58]. Transforms are Cu – S phase-corrected and computed over the *k*-range 1–16 Å^{-1}.

suggesting that the Cu^{II} form of Sco may be involved in maturation of cytochrome oxidase.

The $[Cu_4(SR)_6]^{2-}$ cluster in fact represents a notable success in predictive synthetic bioinorganic chemistry. Almost all biological metal clusters have been structurally characterized in a biological system before they have been synthesized chemically. The $[Cu_4(SR)_6]^{2-}$ cluster, however was first reported in 1976 [54], almost two decades before the first suggestion that it might occur in biological systems [52]. With one notable exception, that of the linear 3-Fe cluster of iron regulatory protein 1 [55], and despite considerable success in reproducing postulated or known biological structures, there are no other examples of predictive success in synthetic metal cluster bioinorganic chemistry.

Clusters with higher nuclearity than $[Cu_4(SR)_6]^{2-}$ are certainly possible, and may also exist in biology [40]. *In vitro* metallothioneins can certainly form a high nuclearity clusters [56], but *in vivo* they may contain predominantly $[Cu_4(SR)_6]^{2-}$ [*cf.* 51]. There are numerous examples of large cuprous thiolate clusters in the chemical literature, and for comparison purposes the discussion is restricted to two examples. Fig. 11 shows the structures of $[Cu_5(SR)_6]^-$ [57] and $[Cu_5(SR)_7]^{2-}$ [58]. These can be regarded as $[Cu_4(SR)_6]^{2-}$ with an added cuprous ion or a [Cu(SR)] moiety, respectively. $[Cu_5(SR)_6]^-$

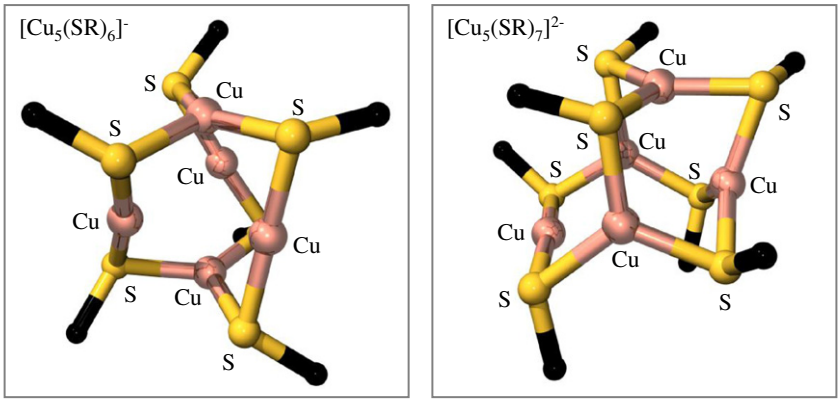

Fig. 11. Structures of $[Cu_5(SR)_6]^-$ [57] and $[Cu_5(SR)_7]^{2-}$ [58].

can be thought of as a cylindrical species with the two ends formed by three-coordinate cuprous ions separated by three two coordinate cuprous ions. Fig. 12 shows the EXAFS Fourier transforms of these species plus that of $[Cu_4(SR)_6]^{2-}$, together with best fits. The experimental data and fit of $[Cu_5(SR)_6]^{-}$ are quite distinct from the simulations presented by Voronova et al. [48], illustrating the importance of experimental data.

6. Conclusions

The coordination chemistry of cuprous copper shows a remarkable degree of plasticity, for both isolated copper sites and for multinuclear clusters. It is widely acknowledged that copper is useful in biological systems because of the accessibility of its one electron redox chemistry. As discussed above, this same chemistry is thought to be responsible for the toxicity of free copper and for the correspondingly rigid homeostasis of the metal. However, redox reactions are carried out by a variety of transition ions so this may not be the sole reason why biology chooses copper, and perhaps the plasticity of the cuprous oxidation state may be an additional important factor. The fictile coordination chemistry of Cu^{I} facilitates the complex series of molecular interactions that allow copper ions to be passed from transporter to a series of chaperones, and finally to the target protein. All of this is likely to occur with relatively low energetic/thermodynamic penalties for changing cuprous copper coordination geometry or cluster size of the transported ion(s).

Acknowledgments

Work at the University of Saskatchewan was supported by the Natural Sciences and Engineering Research Council of Canada, Canada Research Chair awards (G.N.G. and I.J.P.), the University of Saskatchewan, the Saskatchewan Health Research Foundation (SHRF), and the Canadian Institutes for Health Research (CIHR). M.J.P. is supported by CIHR, CIHR-THRUST and SHRF Postdoctoral fellowships.

References

[1] M.M. Pena, J. Lee, D.J. Thiele, A delicate balance: homeostatic control of copper uptake and distribution, J. Nutr. 129 (1999) 1251–1260.
[2] I. Bremner, Manifestations of copper excess, Am. J. Clin. Nutr. 67 (1998) 1069S–1073S.
[3] C. White, T. Kambe, Y.G. Fulcher, S.W. Sachdev, A.I. Bush, K. Fritsche, J. Lee, T.P. Quinn, M.J. Petris, Copper transport into the secretory pathway is regulated by oxygen in macrophages, J. Cell Science 122 (2009) 1315–1321.
[4] T.D. Rae, P.J. Schmidt, R.A. Pufahl, V.C. Culotta, T.V. O'Halloran, Undetectable intracellular free copper: the requirement of a copper chaperone for superoxide dismutase, Science 284 (1999) 805–808.
[5] A. Changela, K. Chen, Y. Xue, J. Holschen, C.E. Outten, T.V. O'Halloran, A. Mondragon, Molecular basis of metal-ion selectivity and zeptomolar sensitivity by CueR, Science 301 (2003) 1383–1387.
[6] D.R. Winge, Copper metalloregulation of gene expression, Adv. Protein Chem. 60 (2002) 51–92.
[7] E. Balatri, L. Banci, I. Bertini, F. Cantini, S. Ciofi-Baffoni, Solution structure of Sco1: a thioredoxin-like protein involved in cytochrome c oxidase assembly, Structure 11 (2003) 1431–1443.
[8] J.C. Williams, C. Sue, G.S. Banting, H. Yang, D.M. Glerum, W.A. Hendrickson, E.A. Schon, Crystal structure of human Sco1: implications for redox signaling by a mitochondrial cytochrome c oxidase "assembly" protein, J. Biol. Chem. 280 (2005) 15202–15211.
[9] B. Delley, An all-electron numerical method for solving the local density functional for polyatomic molecules, J. Chem. Phys. 92 (1990) 508–517.
[10] B. Delley, From molecules to solids with the DMol^3 approach, J. Chem. Phys. 113 (2000) 7756–7764.
[11] A.D. Becke, A multicenter numerical integration scheme for polyatomic molecules, J. Chem. Phys. 88 (1988) 2547–2553.
[12] J.P. Perdew, Y. Wang, Accurate and simple analytic representation of the electron-gas correlation energy, Phys. Rev. B 45 (1992) 13244–13249.
[13] A. Klamt, G. Schüürmann, COSMO: a new approach to dielectric screening in solvents with explicit expressions for the screening energy and its gradient, J. Chem. Soc. Perkin. Trans. 2 (1993) 799–805.
[14] http://ssrl.slac.stanford.edu/exafspak.html.
[15] G.N. George, R.M. Garrett, R.C. Prince, K.V. Rajagopalan, The molybdenum site of sulfite oxidase: a comparison of wild-type and the cysteine 207 to serine mutant using X-ray absorption spectroscopy, J. Am. Chem. Soc. 118 (1996) 8588–8592.
[16] J.J. Rehr, J. Mustre de Leon, S.I. Zabinsky, R.C. Albers, Theoretical x-ray absorption fine structure standards, J. Am. Chem. Soc. 113 (1991) 5135–5140.
[17] J. Mustre de Leon, J.J. Rehr, S.I. Zabinsky, R.C. Albers, Ab initio curved-wave x-ray-absorption fine structure, Phys. Rev. 44 (1991) 4146–4156.
[18] J.J. Rehr, R.C. Albers, Theoretical approaches to x-ray absorption fine structure, Rev. Mod. Phys. 72 (2000) 621–654.
[19] J.E. Penner Hahn, Characterization of "spectroscopically quiet" metals in biology, Coord. Chem. Rev. 249 (2005) 161–177.
[20] J.A. Tang, B.D. Ellis, T.H. Warren, J.V. Hanna, C.L.B. Macdonald, R.W. Schurko, Solid-state ^{63}Cu and ^{65}Cu NMR spectroscopy of inorganic and organometallic copper(I) complexes, J. Am. Chem. Soc. 129 (2007) 13049–13065.
[21] A.S. Lipton, R.W. Heck, W.A. de Jong, A.R. Gao, X. Wu, A. Roehrich, G.S. Harbison, P.D. Ellis, Low temperature ^{65}Cu NMR Spectroscopy of the Cu^{+} site in azurin, J. Am. Chem. Soc. 131 (2009) 13992–13999.
[22] G.N. George, I.J. Pickering, X-ray absorption spectroscopy in biology and chemistry, in: V. Tsakanov, H. Wiedemann (Eds.), Brilliant Light in Life and Materials Sciences, Springer, Dordrecht, NL, 2007, pp. 97–119.
[23] M.J. Pushie, G.N. George, Spectroscopic studies of molybdenum and tungsten enzymes, Coord. Chem. Rev. 225 (2011) 1055–1084.
[24] R.A. Capaldi, Structure and assembly of cytochrome-c-oxidase, Arch. Biochem. Biophys. 280 (1990) 252–262.
[25] A. Atkinson, D.R. Winge, Metal acquisition and availability in the mitochondria, Chem. Rev. 109 (2009) 4708–4721.
[26] Y.-C. Horng, P.A. Cobine, A.B. Maxfield, H.S. Carr, D.R. Winge, Specific copper transfer from the Cox17 metallochaperone to both Sco1 and Cox11 in the assembly of yeast cytochrome c oxidase, J. Biol. Chem. 279 (2004) 35334–35340.
[27] C. Abajian, L.A. Yatsunyk, B.E. Ramirez, A.C. Rosenzweig, Yeast Cox17 solution structure and copper(I) binding, J. Biol. Chem. 279 (2004) 53584–53592.
[28] D.N. Heaton, G.N. George, G. Garrison, D.R. Winge, The mitochondrial copper metallochaperone Cox17 exists as an oligomeric, polycopper complex, Biochemistry 40 (2001) 743–751.
[29] G.S. Siluvai, M. Nakano, M. Mayfield, N.J. Blackburn, The essential role of the Cu(II) state of Sco in maturation of the CuA center of cytochrome oxidase: evidence from H135Met and H135SeM variants of the *Bacillus subtilus* Sco, J. Biol. Inorg. Chem. 16 (2011) 285–297.
[30] L. Banci, I. Bertini, S. Ciofi-Baffoni, T. Hadjiloi, M. Martinelli, P. Palumaa, Mitochondrial copper(I) transfer from Cox17 to Sco1 is coupled to electron transfer, Proc. Natl. Acad. Sci. USA 105 (2008) 6803–6808.
[31] D. Meyerstein, Trivalent Copper. I. A pulse radiolytic study of the chemical properties of the aquo complex, Inorg. Chem. 11 (1971) 638–641.
[32] F.H. Allen, O. Kennard, D.G. Watson, Crystallographic databases: search and retrieval of information from the Cambridge Structural Database, Struct. Correl. 1 (1994) 71–110.
[33] A. Kohner-Kerten, E.Y. Tshuva, Preparation and X-ray characterization of two-coordinate Cu(I) complex of aliphatic thiolato ligand: effect of steric bulk on coordination features, J. Organomet. Chem. 693 (2008) 2065–2068.
[34] K. Fujisawa, S. Imai, S. Suzuki, Y. Moro-oka, Y. Miyashita, Y. Yamada, K. Okamoto, M–S vibrational study in three-coordinate thiolato compounds $(NEt_4)_2[M(SC_6H_4\text{-}p\text{-}X)_3]$ and $(NEt_4)_2[M_4(\mu\text{-}SC_6H_4\text{-}p\text{-}Cl)_6]$: M=Cu(I) and Ag(I), X=Cl and Br, J. Inorg. Biochem. 82 (2000) 229–238.
[35] J.C. Barnes, C.S. Blyth, J.D. Paton, Preparation and thermal analysis of 1,4-oxathiane complexes of silver(I) perchlorate and copper(I) perchlorate. Crystal structures of perchlorato(1,4-oxathiane)silver(I), perchloratobis(1,4-oxathiane)silver(I) and tetrakis(1,4-oxathiane)copper(I) perchlorate, J. Chem. Soc. Pak. 4 (1982) 103–113.
[36] S. Schneider, J.A.S. Roberts, M.R. Salata, T.J. Marks, Mixed diketonate thiolate copper(I) precursors for materials synthesis: control of Cu_2S-forming thermolysis pathways by manipulating Lewis acid and base cluster building blocks, Angew. Chem., Int. Ed. 45 (2006) 1733–1736.
[37] B.T. Op't Holt, K.M. Merz Jr., Insights into Cu(I) exchange in HAH1 using quantum mechanical and molecular simulations, Biochemistry 46 (2007) 8816–8826.
[38] T. Liu, A. Ramesh, Z. Ma, S.K. Ward, L. Zhang, G.N. George, A.M. Talaat, J.C. Sacchettini, D.P. Giedroc, CsoR is a novel *Mycobacterium tuberculosis* copper-sensing transcriptional regulator, Nature Chem. Biol. 3 (2007) 60–68.
[39] T. Nittis, G.N. George, D.R. Winge, Yeast Sco1, a protein essential for cytochrome c oxidase function is a Cu(I)-binding protein, J. Biol. Chem. 276 (2001) 42520–42526.
[40] I.J. Pickering, G.N. George, C.T. Dameron, B. Kurtz, D.R. Winge, I.G. Dance, X-ray absorption spectroscopy of cuprous-thiolate clusters in proteins and model systems, J. Am. Chem. Soc. 115 (1993) 9498–9505.
[41] H.S. Carr, G.N. George, D.R. Winge, Yeast Cox11, a protein essential for cytochrome c oxidase function is a Cu(I)-binding protein, J. Biol. Chem. 277 (2002) 31237–31242.
[42] S. Zeevi, E.Y. Tshuva, Synthesis and X-ray characterization of mono- and polynuclear thiolatocopper(I) complexes: the effect of steric bulk on coordination number and nuclearity, Eur. J. Inorg. Chem. 34 (2007) 5369–5376.
[43] W.W. Seidel, M.D.I. Arias, M. Schaffrath, K. Bergander, A neutral tungsten-eta(2)-alkyne-1-thio ligand forming a homoleptic Werner type complex with Cu(I), Dalton Trans. (2004) 2053–2054.
[44] M.S. Shoshan, E.Y. Tshuva, The MXCXXC class of metallochaperone proteins: model studies, Chem. Soc. Rev. 40 (2011) 5282–5292.
[45] P.J. Hart, A.M. Nersissian, R.G. Herrmann, R.M. Nalbandyan, J.S. Valentine, D. Eisenberg, A missing link in cupredoxins: crystal structure of cucumber stellacyanin at 1.6 Å resolution, Protein Sci. 5 (1996) 2175–2183.
[46] K.R. Brown, G. Keller, I.J. Pickering, H.H. Harris, G.N. George, D.R. Winge, The structures of the cuprous thiolate clusters of the Ace1 and Mac1 transcriptional activators, Biochemistry 41 (2002) 6469–6476.
[47] Z. Xiao, F. Loughlin, G.N. George, G.J. Howlett, A.G. Wedd, The C-terminal domain of the membrane copper transporter Ctr1 from *Saccharomyces cerevisiae* binds four Cu(I) ions

as a cuprous-thiolate polynuclear cluster. Sub-femtomolar Cu(I) affinity of three proteins involved in copper trafficking, J. Am. Chem. Soc. 126 (2004) 3081–3090.
[48] A. Voronova, W. Meyer-Klauke, T. Meyer, A. Rompel, B. Krebs, J. Kazantseva, R. Sillard, P. Palumaa, Oxidative switches in functioning of mammalian copper chaperon Cox17, Biochem. J. 408 (2007) 139–148.
[49] K. Rigby, L. Zhang, P.A. Cobine, G.N. George, D.R. Winge, Characterization of the cytochrome c oxidase assembly factor Cox19 of *Saccharomyces cerevisiae*, J. Biol. Chem. 282 (2007) 10233–10242.
[50] J.A. Graden, M.C. Posewitz, J.R. Simon, G.N. George, I.J. Pickering, D.R. Winge, Presence of a Cu(I)-thiolate regulatory domain in the copper-activated transcription factor amt1, Biochemistry 35 (1996) 14583–14589.
[51] L. Zhang, I.J. Pickering, D.R. Winge, G.N. George, X-ray absorption spectroscopy of cuprous-thiolate clusters in *Saccharomyces cerevisiae* metallothionein, Chem. Biodivers. 5 (2008) 2042–2049.
[52] C.T. Dameron, D.R. Winge, G.N. George, M. Sansone, S. Hu, D. Hamer, A copper thiolate polynuclear cluster in the Ace1 transcription factor, Proc. Natl. Acad. Sci. USA 88 (1991) 6127–6131.
[53] G.N. George, J. Hilton, C. Temple, R.C. Prince, K.V. Rajagopalan, The structure of the molybdenum site of dimethylsulfoxide reductase, J. Am. Chem. Soc. 121 (1999) 1256–1266.
[54] I.G. Dance, J.C. Calabrese, The crystal and molecular structure of the hexa-(μ_2 benzenethiolato)tetracuprate(I) dianion, Inorg. Chim. Acta. 19 (1976) L41–L42.
[55] J. Gailer, G.N. George, I.J. Pickering, R.C. Prince, P. Kohlhepp, D. Zhang, F.A. Walker, J.J. Winzerling, Human cytosolic iron regulatory protein 1 contains a linear iron–sulfur cluster, J. Am. Chem. Soc. 123 (2001) 10121–10122.
[56] V. Calderone, B. Dolderer, H.-J. Hartmann, H. Echner, C. Luchinat, C. Del Bianco, S. Mangani, U. Weser, The crystal structure of yeast copper thionein: the solution of a long-lasting enigma, Proc. Natl. Acad. Sci. USA (2005) 51–56.
[57] G.A. Bowmaker, G.R. Clark, J.K. Seadon, I.G. Dance, The formation and structural chemistry of the hexa(μ-*t*-butylthiolato) pentacuprate(I) cage anion with triethylammonium and tetraethylammonium cations, Polyhedron 3 (1984) 535–544.
[58] I.G. Dance, The hepta(μ_2-benzenethiolato)pentacuprate(I) dianion; X-ray crystal and molecular structure, J. Chem. Soc., Chem. Commun. (1976) 103–104.